*Int. J. Electrochem. Sci.*, 7 **(2012)** 12856 - 12869

International Journal of
ELECTROCHEMICAL
SCIENCE
www.electrochemsci.org

# Nickel Electrodeposition from Protic Ionic Liquids Based on Carboxylate Anions as Electrolyte: I. Electrodeposition from 2-hydroxyethyl Ammonium Formate.

*E. Cuara-Diaz.*[1], *G. Brisard* [2], *G. Trejo*[1], *Y.Meas*[1], *R. Ortega-Borges*[1,*]

[1] Centro de Investigación y Desarrollo Tecnológico en Electroquímica (CIDETEQ), Parque Tecnológico Querétaro-Sanfandila. 76703 Pedro Escobedo, Qro, México.
[2] Faculté de Sciences Université de Sherbrooke, 2500, Blv. de l'Université Sherbrooke, Sherbrooke (PQ) Canada J1K 2R1
[*]E-mail: rortega@cideteq.mx

*Received:* 27 September 2012 / *Accepted:* 17 October 2012 / *Published:* 1 December 2012

---

Ni electrodeposition from a protic ionic liquid based on carboxylated anions, 2-hydroxyethyl ammonium formate (2HEAF), was studied in order to evaluate the feasibility to obtain deposits with well-controlled properties and also to determine the influence of the electrodeposition conditions on these properties. Results show that nickel is electrodeposited from this non-aqueous medium following an instantaneous nucleation mechanism as a pure, compact and uniform deposit, composed of nanocrystallites with size ranging from 18 nm to 23 nm, without the use of additives or tensioactive agents, contrary to what is required to obtain similar deposits from aqueous electrolytes.

---

**Keywords:** protic ionic liquids; nickel electrodeposition; nanomaterials.

## 1. INTRODUCTION

In the last two decades the interest in the study of nanocrystalline materials has been increased due to their both real and potential applications in several technological fields, associated to the improvement of their chemical and physical properties reflected by example in an increase in catalytic activity or in better mechanical performances [1,2]. The enhancements of the properties of these materials are associated to the changes in reactivity due to the change in scale of size when materials are formed by nanoparticles.

Several preparation processes have been developed to try to obtain nanocrystalline materials; unfortunately most of these produce bulk, microparticle or porous structures without improve in their reactivity and even with poorer mechanical properties or with a limited chemical resistance to corrosion when compared with bulked or microstructured materials.

In other hand, it has been demonstrated that electrodeposition is an effective technique to produce nanocrystalline deposits of metallic or composite materials with numerous advantages as to allow to obtain deposits with the same basic experimental setup than those used to produce bulked or microstructured material; electrodeposition allows also to control both the thickness and the crystal orientation of the electrodeposited material by controlling the deposition parameters as current density during the electrodeposition process; in addition, films produced by electrodeposition are generally compact, homogenous and with a microstructured texture function of the experimental conditions [3,4].

A very important case of technological interest is the electrodeposition of nanocrystalline nickel (Ni) which is generally used as electrode material to increase the performance of cathodic processes, to generate new classes of materials and also because the presence of Ni in several material improves properties as corrosion and wear resistant and it is widely used in solar energy generation devices, catalysis, sensors, energy and media storage [5-7]. However, some limitations in the Ni production are observed from the reported aqueous electrochemical methods. Normally it is quite difficult to obtain nanocrystalline films of Ni without the use of tensioactive agents or without the electrochemical reduction of the electrolyte into hydrogen as competitive reaction which leads to low current efficiencies and low texture quality of the deposits [8]. In addition, another disadvantage associated to electrodeposition is related to the ecological aspects of them because of electrodeposition processes typically require specific pre-treatments and cleaning steps consuming additional energy and generating wastes that have to be treated [9]. For these reasons, permanent efforts are carried out to develop new technologies allowing obtaining well controlled electrodeposits and that can reduce also the costs of production by reducing the number of steps and with a minimal generation of effluents.

In recent years room temperature ionic liquids (RTIL) have attracted considerable attention because these new solvents offer interesting possibilities related to their use as ecologically friendly solvents in chemical and electrochemical processes and in applications taking advantage of their properties as liquid material [10-14]. Since RTIL generally have several distinctive properties, such as wide electrochemical windows, high conductivity compared to non-aqueous strong electrolytes and negligible vapor pressure[15-18], they are expected to be an alternative media for the electrodeposition of metals in both micro and nano scale [13, 19-22]. Concerning the electrodeposition of nanocrystalline Ni, it has been successfully achieved in some RTIL based on imidazolium, chloroaluminate cations or even in some new media as deep eutectic solvents as choline chloride based solvents [23-25]. Unfortunately, these electrolytes requires the use of additives and complexing agents in order to stabilize the pH during the electrodeposition process or the feasibility to be applied in electrodeposition process is greatly reduced due to their intrinsic toxicity and instability in contact with water [13, 26-33]

In this work the use of 2-hydroxyethyl ammonium formate (2HEAF) as a new solvent for Ni electrodeposition is studied, 2HEAF is selected due to its chemical stability in presence of water; 2HEAF also exhibit desirable physicochemical properties such as high conductivities, low viscosities and a lower toxicity for electrochemical application without the observed disadvantages of ionic liquids based in chloroaluminates, imidazolium or pyridinium ions.

## 2. EXPERIMENTAL

2HEAF was synthetized by an acid-base neutralization reaction mixing equimolar quantities of formic acid 94% (Sigma-Aldrich) and ethanolamine 99.99% (J.T. Baker). Reactants were added dropwise in a thermoregulated glass cell under Ar atmosphere [34, 35]. All reactants were analytical grade and were used without previous purification because the chemical stability of the precursors and the obtained 2HEAF is not influenced by the presence of water. Due to its highly exothermic nature, the neutralization reaction was carried out at 5 °C under vigorous magnetic stirring to avoid the formation of by-products or decomposition products such as N-(2-hydroxyethyl) formamide which is formed by the local increment of the temperature at the interface of the precursors as previous results shown. In order to remove the residual water, the obtained 2HEAF was dried under vacuum overnight at 50 °C and -30inHg. The final $H_2O$ content was determined to be lower than 100 ppm by a Karl Fischer titration (KF 787 Titrino Metrohm). The purity of the 2HEAF was verified by FTIR (Thermo Nicolet Nexus 870) and H-NMR (Avance 600MHz, 14.1T, Bruker). No by-products or decomposition products were evidenced.

The study of the electrodeposition of Ni from 2HEAF was carried out by cyclic voltammetry using 10 and 22 mM of Ni(II) solutions prepared by dissolving $NiSO_4 \cdot 6H_2O$ 99.9% (J. B. Baker) in freshly synthetized and dried 2HEAF. The electrochemical measurements were carried out with a 273A EG&G Potenciostate/Galvanostate Princeton Applied Research in a conventional three-electrode thermoregulated glass cell in an Ar filled glove box with a $H_2O$ concentration lower than 1ppm. Ni deposits at controlled potential were carried out during 5, 10, 15, 20 and 60 minutes at a controlled potential of -675 mV, corresponding to the conditions where the electrodeposition process is limited by only by mass transfer; during the experiments, the temperature of the electrochemical system was fixed at 25 °C with the aid of a thermoregulated bath filled with silicon oil. Mirror polished polycrystalline gold (Au) disk electrodes ($1.96x10^{-3}$ $cm^2$) 99.999% were employed as working electrodes in all the electrochemical experiments; all the reported potentials were referenced to a silver (Ag) wire 99.99% quasi-reference electrode which was separated from the main electrolyte by a single junction crystal chamber filled with pure 2HEAF and enclosed by a porous Vycor glass; finally a platinum (Pt) mesh electrode was used as a counter electrode.

The Ni nucleation process in the 10mM $NiSO_4$ solution was studied from the current density transients at constant potential of -500, -550, -675 and -850 mV vs Ag. The electrodeposits were washed with pure water and dried in air prior to be characterized by a scanning electron microscope (SEM, JEOL JSM5400LV) and energy dispersive spectrometer analysis (EDS, Kervex Delta Plus). The thickness of the electrodeposited $Ni^0$ was measured by a Veeco Dektak 6M profilometer controlled by its software v8.30.005. The X-ray diffraction (XRD) experiments were carried out with a Bruker D8 Advance type diffractometer, using a Cu Kα radiation (λ = 1.3932 Å). The diffraction pattern was scanned by small angles > 1 degree.

## 3. RESULTS AND DISCUSSION

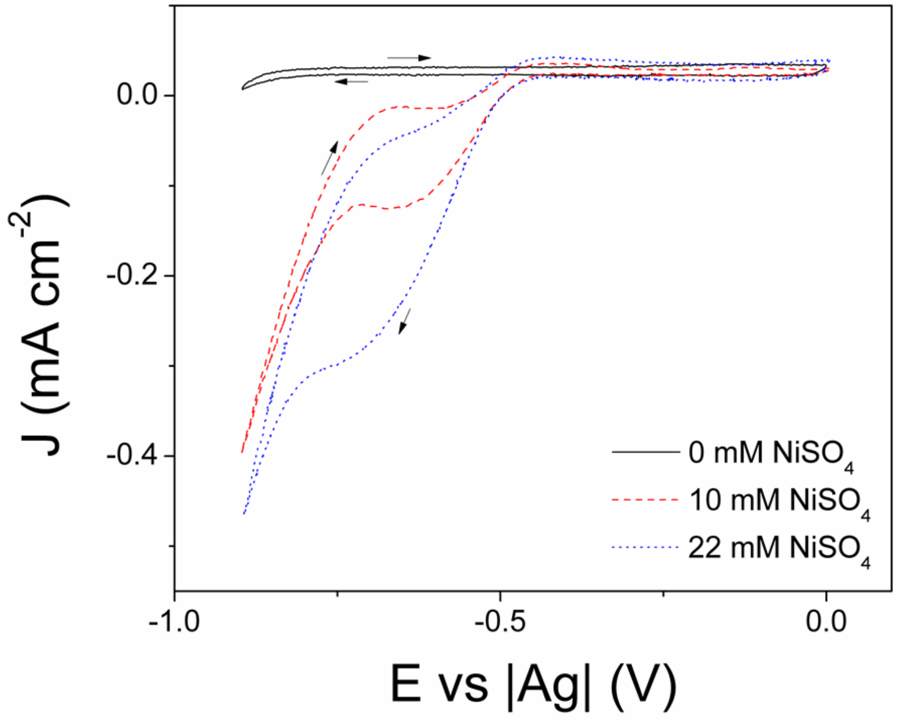

**Figure 1.** Cyclic voltammetry, showing the electrochemical window for $NiSO_4$ in 2HEAF using a polycrystalline gold electrode at 20 mV $s^{-1}$.

Figure 1 shows the electrochemical behavior of a polycrystalline Au electrode immersed in solutions containing 0 mM, 10 mM, 22 mM Ni(II) in 2HEAF, at 20 mV $s^{-1}$. As seen, an electrochemical window of 920 mV is observed in absence of electro-active species of Ni(II). In this case, the cathodic limit is associated to a two-step reduction process of the ethanol ammonium ion: the first process involves the adsorption of the ethanolammonium ion into the electrode surface (1) and the second process corresponding to the electrochemical reduction of the adsorbed ion to produce ethanolamine and molecular hydrogen (2); these reactions are proposed in the basis of previous results obtained by differential electrochemical mass spectrometry (DEMS); the nature of the evolved gases was confirmed by these results. The anodic limit is also associated to a two-step oxidation process starting with the ion formate adsorption (3) continued with the electrochemical oxidation of the adsorbed ions liberating protons into the solution and carbon dioxide (4) [36]. In presence of electroactive spices of Ni(II), a well-defined cathodic signal appears at -500 mV vs |Ag| with a current density directly dependent on the Ni(II) concentration; this signal is associated to the electrochemical reduction of Ni (II) to $Ni^0$ and shows that in the studied ionic liquid, the electrochemical reduction of Ni(II) is carried out by a single step process. Similar results are observed when nickel is electrodeposited from aqueous solutions; for example in the classical nickel electrodeposition baths, the process is also carried out by a well-known one step process involving two electrons [37, 38]; a plateau is observed at a potential of -650 mV vs |Ag| associated to a typical diffusion controlled process behaviour.

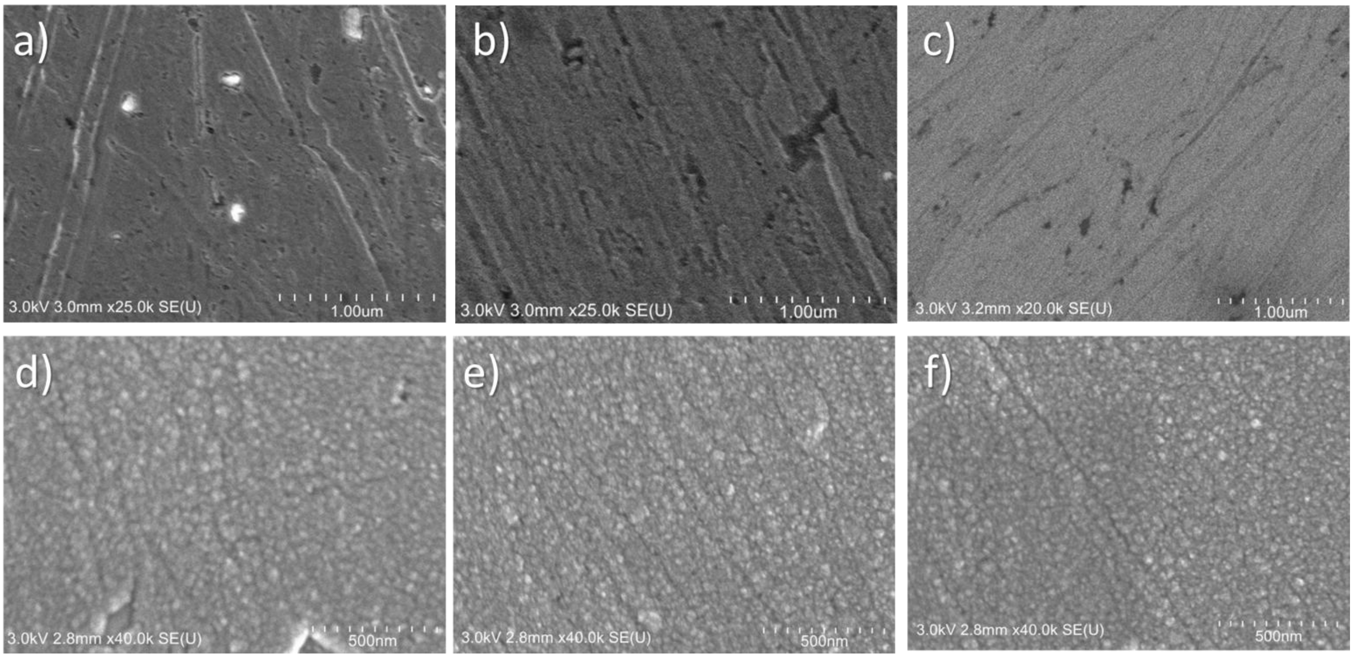

**Figure 2.** SEM images of the growth process of the electrochemical deposition on a polycrystalline gold electrode after (a) 0, (b) 5, (c) 10, (d) 15, (e) 20, and (f) 60 min.

A second signal started at a potential of -720 mV vs |Ag|. This new process correspond to the electrolyte reduction; after reversing the potential scan direction, no oxidation of $Ni^0$ formed is observed, indicating that in these experimental conditions the $Ni(II)/Ni^0$ system behaves as an irreversible electrochemical system, nevertheless the current stabilized at -680mV, and continued declining after -570 mV, this signals indicate that the electrochemical reduction of nickel continue even after changing the direction of the potential scan; this behavior have been observed for some electrodeposition process and it is typical behavior of a metallic electrodeposition process involving nucleation [39].

$$[\mathrm{HO\text{-}CH_2\text{-}CH_2\text{-}NH_3}]^+ \rightarrow [\mathrm{HO\text{-}CH_2\text{-}CH_2\text{-}NH_3}]^+_{(ads)} \quad (1)$$

$$2\,[\mathrm{HO\text{-}CH_2\text{-}CH_2\text{-}NH_3}]^+_{(ads)} + 2e^- \rightarrow 2\ \mathrm{HO\text{-}CH_2\text{-}CH_2\text{-}NH_2} + \mathrm{H_2}\uparrow \quad (2)$$

$$[\mathrm{HCOO}]^- \rightarrow [\mathrm{HCOO}]^-_{(ads)} \quad (3)$$

$$2\,[\mathrm{HCOO}]^-_{(ads)} \rightarrow 2\ \mathrm{CO_2} + 2\ \mathrm{H}^+ + 2e^- \quad (4)$$

Ni electrodeposits at controlled potential were obtained on gold electrodes from a 10 mM $NiSO_4$ solution in 2HEAF; a constant potential of -675 mV vs |Ag| was imposed at several depositions times ($t_{deposition}$) in order to evaluate the influence of the deposition time on the morphological properties of the deposits observed by SEM.

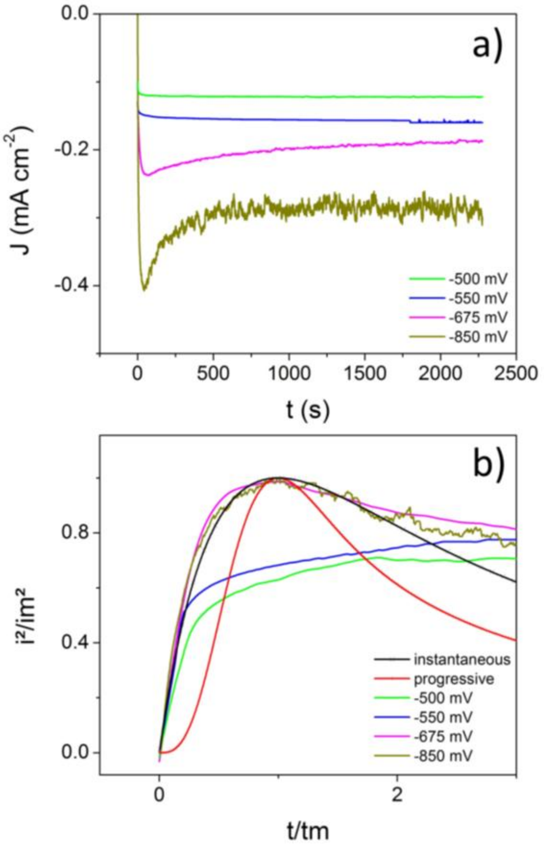

**Figure 3.** Chronoamperometric response during deposition of Ni in a 10 mM $NiSO_4$ solution of 2HEAF. a) Experimental data from four different applied pulse potentials. b) Normalized experimental transients compared with both instantaneous and progressive nucleation models.

Results are shown in figure 2. Micrograph in Figure 2a corresponds to the polished polycrystalline gold electrode substrate without any specific treatment. In figure 2b and 2c ($t_{deposition}$= 5 and 10 min) no visible changes on the substrate were observed. At longer deposition times ($t_{deposition}$= 15, 20 and 60 min, Figures 2d, 2e and 2f, respectively) a metallic, homogeneous deposit formed by spherical particles is clearly evidenced, the observed morphology is similar to that observed for nickel electrodeposits obtained by Abbott and coworkers [31] and by H. Yiang et al [40] from a $NiSO_4$ solution in a mixture of chloline - chloride urea, a deep eutectic ionic liquid. Similar morphologies are also observed when nickel is electrodeposited from typical aqueous electrodeposition baths in the presence of additives and complexing species [37, 38, 41, 42]. A visual inspection to the electrode shows that an increase in the thickness of the electrodeposited Ni changes the color and qualitative aspect of the obtained deposits from a bright metallic gold to a near black deposit, indicating that deposits are formed by dispersed small particles.

The electrocrystallization of Ni in 2HEAF was studied in a similar way to that used in aqueous electrolytes, assuming that the nucleation process can be either an instantaneous or progressive process, and the growth mode can involve one, two, or three-dimensional growth, with needles, disks cones or hemispheres shapes. In order to determinate the type of nucleation process involved in Ni deposition, it is assumed that the crystal growth is carried out according to a three-dimensional model with predominant hemispheres shapes. This assumption is supported with the obtained SEM images which also show the existence of hemispheres evenly distributed over the electrode surface. The analytical expression used for the instantaneous (5) and progressive(6) nucleation were defined by Scharifker and coworkers [43, 44], these equations define multiple nucleation phenomena followed by diffusion-controlled growth of three-dimensional islands.

$$\frac{i^2}{i_m^2} = 1.9542\frac{t_m}{t}\left[1 - \exp\left(-1.2564\frac{t}{t_m}\right)\right]^2 \tag{5}$$

$$\frac{i^2}{i_m^2} = 1.2254\frac{t_m}{t}\left[1 - \exp\left(-2.3367\frac{t^2}{t_m^2}\right)\right]^2 \tag{6}$$

Where “$i_m$“ is the maximum current density in the current density transient and “$t_m$” is the time at this maximum point.

Figure 3 shows the chronoamperometric response and the normalized representation of the experimental current density transient with $t_m$ = 70.8959 s and $i_m$ = -0.2364 mA $cm^{-2}$. For comparison, the calculated curves for instantaneous nucleation and progressive nucleation are also drawn. It is evident that for shorter times, $t_m$, the experimental curve fits the instantaneous nucleation model, similarly to that observed on amine based ionic liquids [40, 45]. At times higher than 2 $t_m$ and for the higher studied potentials, the experimental curve started to deviate from the behavior predicted with this model; this fact may be explained in account of the secondary cathodic reactions involved in the reduction of 2HEAF, with simultaneous gas evolution during generation of Ni crystals producing also the observed instability of the current response at these conditions .

The instantaneous nucleation process for Ni electrodeposited from 2HEAF allows to explain the smooth and homogeneous morphology of the deposits observed by SEM. This effect of the nucleation mechanism on the morphology is similar to those observed for Ni electrodeposited when an instantaneous nucleation process is involved whether the electrodeposition is performed in aqueous medium [42] or in ionic liquid [40] and is quite different of the morphology of nickel electrodeposited from imidazolium-based ionic liquids [46, 47] where deposits are formed by a progressive nucleation mechanism and nodular, no homogeneous and highly porous deposits are obtained.

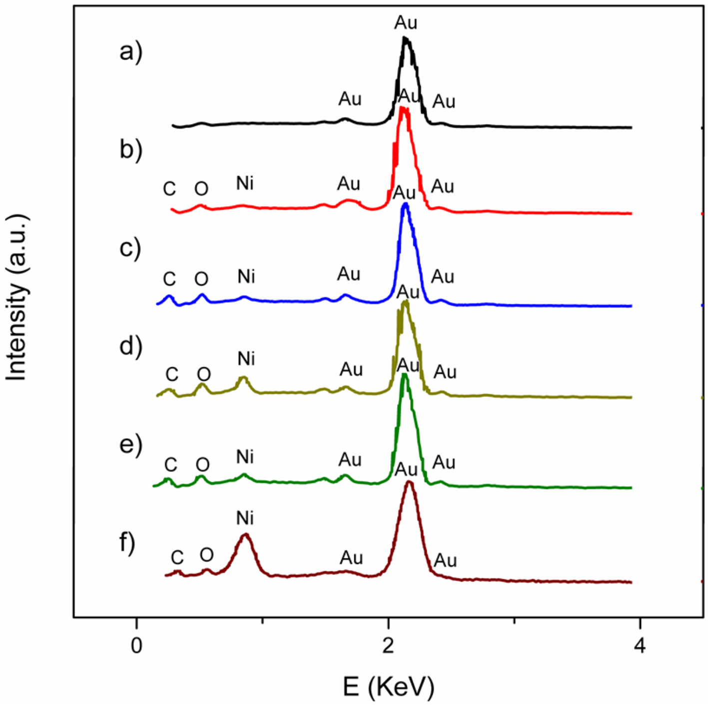

**Figure 4.** EDS analysis of the electrodeposited nickel over the polycrystalline gold electrode after (a) 0, (b) 5, (c) 10, (d) 15, (e) 20, and (f) 60 min of reaction time.

Figure 4 shows results of the EDS analysis of the surface of the electrodeposited Ni. Peaks associated to the substrate (Au signal) are always observed because of Ni is electrodeposited as a very thin film. In all the cases only the presence of Au and Ni is observed confirming the formation of thin Ni films even at the shortest times where is not possible to determinate the structural changes of the substrate surface by SEM analysis due to the thinness of the $Ni^0$ film. The EDS analysis also show the presence of two unexpected elements, Carbon and Oxygen, both of these elements were found only in the surface and most likely came from the exposure of the Ni deposits to the atmosphere. Figure 5 shows the time variation of the thickness for the electrodeposited Ni measured by profilometry. As expected, the Ni layer thickness increases linearly with the deposition time and allow to explain that for shorter deposition times it is difficult to evidence the presence of Ni by SEM and EDS because of the low thickness (below 50 nm) of the electrodeposited Ni. According to M. Schlesinger [48] et al, by using the equations (7) and (8), it was possible to determinate the efficiency of the reaction employing both the electrodeposit thickness and the experimental current transients, estimating an efficiency of 85%, this is probably due to a decreasing selectivity result of the simultaneous electrochemical reduction of the electrolyte.

$$Q_{faradaic} = \frac{AL\rho M}{nF} I \cdot t \qquad (7)$$

$$\%_{eff} = \frac{100 \cdot Q_{faradaic}}{Q_{experimental}} \qquad (8)$$

Where ”$Q_{faradaic}$” is the estimated charge used to generate the Ni deposits, “$Q_{experimental}$” is the experimental charge obtained from the integer value of the current during the deposition time, “A” is the electrode area, “L” the electrodeposit thickness, “ρ” the Nickel density (8.907 gr mol-1), “M” is the molecular weight of Ni, “n” is transferred electrodes, “F” the faraday constant (96500 C mol-1), “I” is the current during the process and “t” the time.

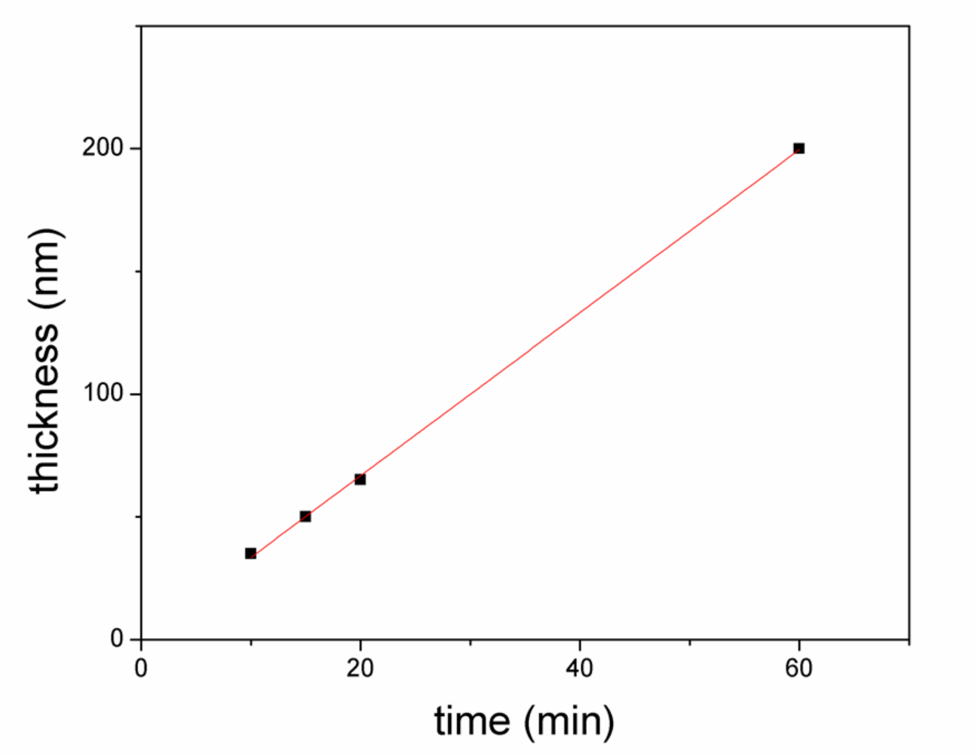

**Figure 5.** Layer thickness of the electrodeposited $Ni^0$ as function of time.

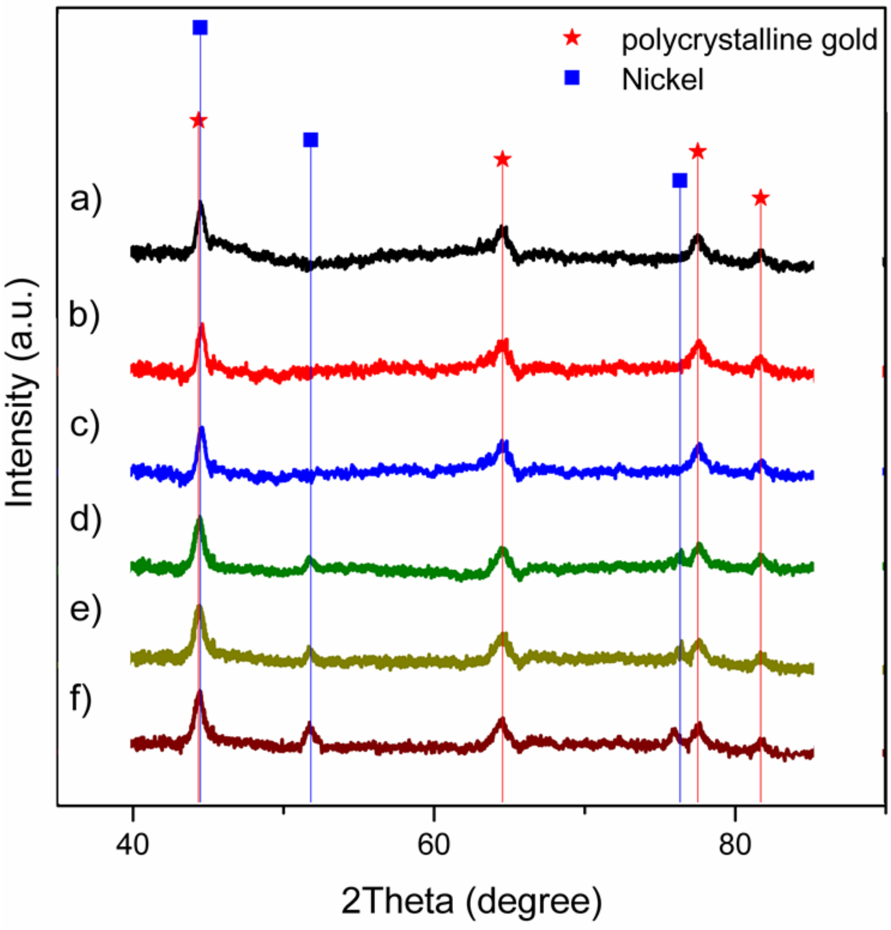

**Figure 6.** XRD patterns after (a) 0, (b) 5, (c) 10, (d) 15, (e) 20, and (f) 60 min of reaction time of deposits.

Figure 6 shows the XRD spectra of the obtained deposits. Sharp diffraction Ni peaks are observed at 51.847 and 76.372 degrees for deposits obtained at deposition times longer than 15 min, indicating the high crystalline character of the electrodeposited Ni. The intensities of the Ni peaks increase when the deposition time is increased. The crystallite size of the electrodeposited Ni was calculated from the major diffraction peak using the Scherrer formula (9) [49,50],

$$D = 0.89\,\lambda\,(\beta \cos\theta)^{-1} \qquad (9)$$

Where $\lambda$ is the wavelength of the X-ray (1.3932 Å) for Cu radiation, $\beta$ is the full width at half maximum of the prominent intensity peak using the 100% relative intensity peak, and $\theta$ the peak position. Table 1 shows that after 15 minutes of reaction time, the estimated grain sizes were found to be about 21 nm with a dispersion value decreasing as the reaction time evolved, archiving values up to 2.0528 showing that deposits are formed by homogenous nanosized particles which can be growth without agglomeration; it is interesting to remark that nickel electrodeposits formed by crystallites as small as 15 nm, have been obtained from choline-based deep eutectic ionic liquids, nevertheless electrodeposition in these media requires the use of special operation parameters or the presence of complexing agents that make process control difficult [51, 52].

**Table 1.** The obtained crystal sizes of the electrodeposited Ni estimated by the Scherrer equation.

| Time (min) | N. Total | Mean (nm) | Standard deviation |
|---|---|---|---|
| 15 | 6 | 20.8544 | 4.72723 |
| 20 | 6 | 20.714 | 2.49237 |
| 60 | 6 | 20.9357 | 2.05283 |

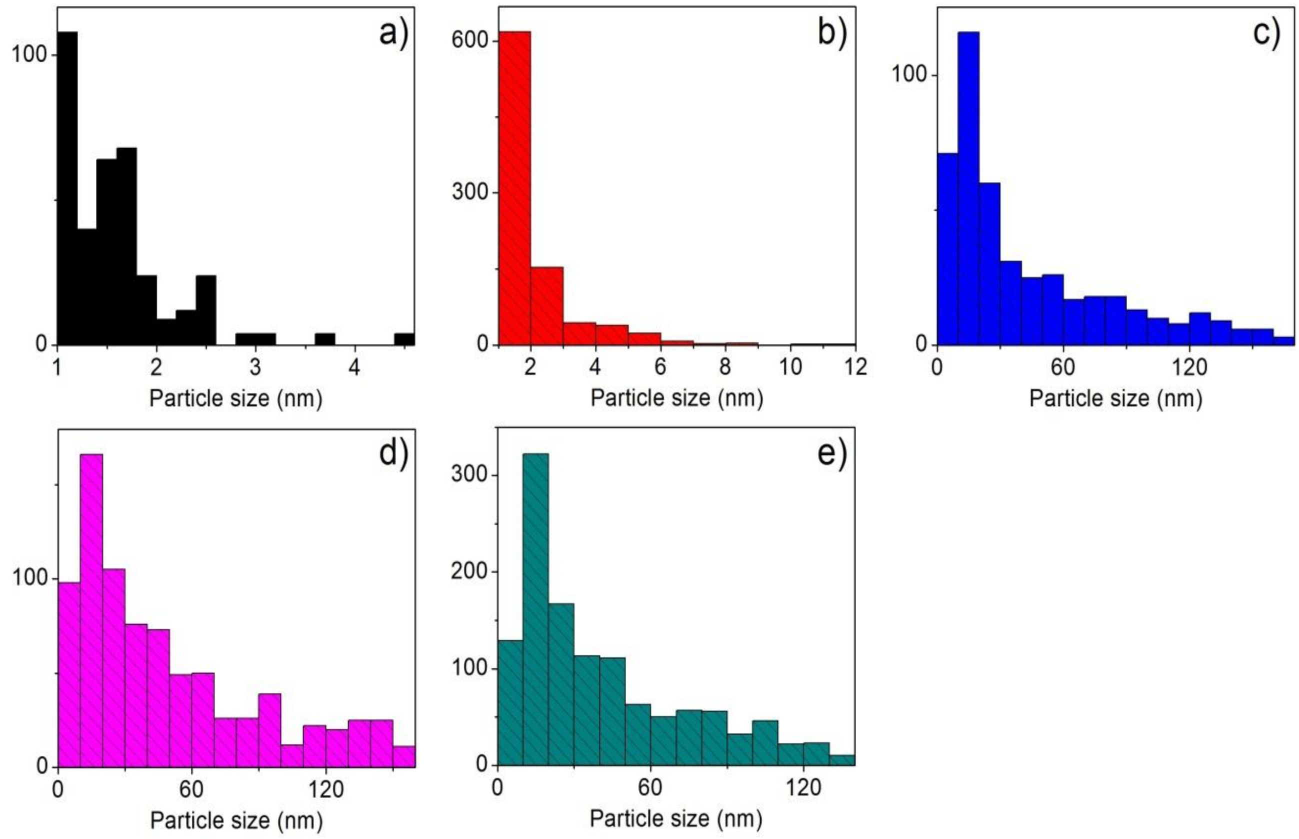

**Figure 7.** Particle size distribution histograms after a deposition time of: a) 5min b) 10min c) 15min d) 20min e) 60 min.

The obtained particles were also studied using image analysis software from the National Institutes of Health, USA (ImageJ v1.46r) which help us confirms that the obtained particles were indeed nanosized crystals with a hemispherical morphology. Figure 7 shows the statistical analysis of the particles sizes obtained from this software, as seen, for 5 and 10 minutes of reaction, the obtained crystals are not bigger than 6 nm height with a predominant size of 2 nm. For longer deposition times, the analysis showed that predominating sizes are 20 nm; however, Table 2 shows that the obtained mean values of the measured crystals sizes are 47 nm with a very high dispersion value of 40 nm. These values were probably obtained due to the incapacity of the software to distinguish between a crystal and an agglomeration of them.

**Table 2.** The obtained crystal sizes of the electrodeposited Ni estimated by the image analysis software.

| Time (min) | N. Total | Mean (nm) | Mode (nm) | Standard deviation |
|---|---|---|---|---|
| 5 | 365 | 1.614 | 1.132 | 0.59788 |
| 10 | 890 | 1.9979 | 1.122 | 1.2816 |
| 15 | 449 | 45.9964 | 19.029 | 38.48956 |
| 20 | 823 | 51.4564 | 19. 542 | 39.2014 |
| 60 | 1201 | 43.5483 | 19.661 | 31.2131 |

## 4. CONCLUSIONS

Results shows that thin layers of nanocrystalline $Ni^0$ can be successfully obtained by electrodeposition on a polycrystalline gold electrode from $NiSO_4$ solutions in 2HEAF similarly that in aqueous media, but in the absence of additives or complexing agents. The results also shows that the electrochemical reduction of Ni(II) to $Ni^0$ occurs under an instantaneous nucleation model, the efficiency of the process was estimated to be 85%. The morphological characterization shows that the electrodeposited Ni surface is similar to those obtained from ionic liquids formed by mixtures of choline chloride- urea, covering homogeneously the electrode surface with a thin layer constituted only by $Ni^0$; the thickness and crystal size of the Ni deposits are dependent on the deposition time. In our experimental conditions, Ni deposits are formed by hemispherical nanoparticles 21 nm sized; the thickness of the film can be accurately controlled adjusting the reaction time of the electrodeposition process. These results demonstrate the feasibility to obtain nanocrystalline Ni deposits from a new and competitive process based in the use of a protic ionic liquid based on carboxylated anions, the 2-hydroxyethyl ammonium formate (2HEAF) in the absence of additives and with better mrphologial properties that deposits obtained from imidazolium-based ionic liquids.

## ACKNOWLEDGEMENTS

The financial support provided by CONACYT (Mexico), project CB 2011-168032 and the Engineering Research Council of Canada (NSERC) are gratefully acknowledged.

## References

1. C. C. Koch, *Nanostructured Materials, Processing, Properties, and Applications*, William Andrew, Releigh, North Carolina (2007).
2. B. Q. Han, E. J. Lavernia and F. A. Mohamed, *Rev. Adv. Mater. Sci*, 9, (2005), 1.
3. G. Staikov, *Electrocrystallization in nanotechnology*, Wiley-VCH, Weinheim (2007).
4. G. Cao, *Nanostructures and nanomaterials. Synthesis, Properties, and Applications*, Imperial college press, London (2004).
5. S. K. Mukhtarov, V. A. Valitov and N. R. Dudova, *Rev. Adv. Mater. Sci*, 25, (2010), 219.
6. P. Moriarty, *Rep. Prog. Phys.*, 64, (2001), 297.
7. R. L. Edson, *Nanostructured Materials for Electrochemical Energy Production and Storage,* Springer Science (2009).
8. L. Peraldo, B. Bozzini, C. Mele and L. D'Urzo, *Int. J. Electrochem. Sci.*, 3, (2008), 356
9. M. Li, S. Luo, Y. Qian, W. Zhang, L. Jiang and J. Shen, *J. Electrochem. Soc.*, 154, (2007), D567.
10. M. J. Earle and K. R. Seddon, *Pure Appl. Chem*, 72, (2000), 1391.
11. N. D. Khupse and K. Anil, *Indian J. Chem. Sec A*, 49A, (2010), 635.
12. R. M. Douglas, M. Forsyth, P. C. Howlett, J. M. Pringle, J. Sun, G. Annat, W. Neil and E. I. Izgorodina, *Acc. Chem. Res.*, 40, (2007), 1165.
13. H. Ohno, *Electrochemical aspects of ionic liquids*, John Wiley & Sons, Inc., Hoboken, New Jersey (2005).
14. P. Wasserscheid and T. Welton, *Ionic Liquids in Synthesis*, Wiley-VCH Verlag GmbH & Co. KGaA, Weinheim (2008).
15. K. Binnemans, *Chem. Rev.*, 105, (2005), 4148.
16. F. Zhou, Y. Liang and W. Liu, *Chem. Soc. Rev*, 38, (2009), 2590.
17. M. Galinski, A. Lewandowski and I. Stepniak, *Electrochem. Acta*, 51, (2006), 5567.
18. C. A. Angell, W. Xu, M. Yoshizawa and J. P. Belieres, *Molten Salts*, 79, (2003), 1.
19. F. Enders, D. MacFarlane and A. Abbot, *Electrodeposition from ionic liquids*, WILEY-VCH Verlag GmbH & Co., Weinheim (2008).
20. M. J. Earle and K. R. Seddon, *Pure Appl. Chem*, 72, (2000), 1391.
21. K. E. Johnson, *Electrochem. Soc. Interface*, Spring, (2007), 38.
22. J. F. Huang, L. H. and S. Dai, *J. Electrochem. Soc.*, 153, (2006), J9.
23. M. H. Allahyarzadeh, B. Roozbehani, A. Ashrafi, S. R. Shadizadeh and A. Seddighian, *J. Electrochem. Soc.*, 159, (2012), D473.
24. A. Kokorin, *Ionic Liquids: Theory, Properties, New Approaches*, InTech, Rijeka, Croatia (2011).
25. G. Li-Xia, W. Li-Na, Q. Tao and Y. Jiang, *Acta Phys. -Chim. Sin.*, 28, (2012), 111.
26. L. E. Barrosse-Antle, A. M. Bond, A. M. O'Mahony, E. I. Rogers and D. S. Silvester, *Chem. Asian J.*, 5, (2010), 202.
27. P. J. Scammells and J. L. Scott, *Aust. J. of Chem.*, 58, (2005), 155.
28. M. Deetleefs and K. R. Seddon, *Chim. Oggi*, 24, (2006), 16.
29. Z.-B. Zhou, H. Matsumoto and K. Tatsumi, *Chem. European J.*, 12, (2006), 2196.
30. A. P. Abbott, G. Capper, K. J. McKenzie and K. S. Ryder, *J. Electroanal. Chem.*, 599, (2007), 288.
31. A. P. Abbott, K. Ttaib, G. Frisch, K. J. McKenzie and K. S. Ryder, *Phys. Chem. Chem. Phys.*, 11, (2009), 4269.
32. A.-M. Popescu, V. Constantin, A. Cojocaru and M. Olteanu, *Revista De Chimie*, 62, (2011), 206.
33. E. Gomez, E. Pellicer and E. Valles, *J. Electroanal. Chem.*, 517, (2001), 109
34. B. Nuthakki, T. L. Greaves and I. Krodkiewska, *Aust. J. of Chem.*, 60, (2007), 21.

35. P. Wasserscheid, A. Bosmann and V. Hal, Halogen-Free Ionic Liquids, in Patent Application Publication, L. Innovar Editor, US 2005/0070717 A1, United States, p. 14 (2005).
36. M. Iglesias, A. Torres, R. Gonzales-Olmos and S. D., *J. Chem. Thermodynamics*, 40, (2008), 119.
37. W. Davison and J. A. Harrison, *J. Electroanal. Chem.*, 36, (1972), 399.
38. M. Fleischmann and A. Saraby-Reintjes, *Electrochem. Acta*, 29, (1984), 69.
39. G. Trejo et al., *J. Appl. Electrochem.*, 31 (2001) 685.
40. H. Yang et al., *Appl. Surf. Sci.*, 257 (2011) 9094.
41. F. Ebrahimini, Z. Ahmed, *Mat. Charac.*, 49 (2003) 373.
42. M. Torabi, A. Dolati, *J. Appl. Electrochem.*, 40 (2010) 1941.
43. Scharifker B and G. Hills, *Electrochem. Acta*, 28, (1983), 879.
44. E. Noam and E. Moshe, *J. Biomed. Mater. Res. A*, 80A, (2007), 621.
45. L. X. Gao et al., *Acta Phys. Chin Sin.*, 28 (2012) 111.
46. A. Lahiri, R. Das., *J. Appl. Electrochem.*, 40 (2010) 1991.
47. M. J. Deng et al., *Electrochim. Acta.*, 53 (2008) 5812.
48. M. Schlesinger and M. Paunovic, Modern Electroplating, Fifth Edition, John Wiley & Sons, Inc. (2010).
49. H. Klung and L. Alexander, X-Ray diffraction procedures, Wiley, New York (1962).
50. J. Zhu, Y. Koltypin and A. Gedanken, *Chem. Mater.*, 12, (2000), 73.
51. S. Handy, Applications of Ionic Liquids in Science and Technology, Middle Tennessee State University, Tennessee, USA (2011).
52. A. Florea et al., *Surf. Interface Anal.*, 42 (2010) 1271.